Disponible en: https://www.redalyc.org/articulo.oa?id=56582396011

Regional extreme rainfall estimation in the Middle Black Sea Region, Turkey

Kadri YUREKLI[1]*, Melih ENGINSU[2] and Muberra ERDOGAN[1]

[1]*University of Gaziosmanpasa, Agriculture Faculty, Department of Biosystem Engineering, Tokat, Turkey.*
[2]*Black Sea Agricultural Research Institute, Samsun, Turkey.*
*Corresponding author; email: kadriyurekli@yahoo.com

RESUMEN

Las probabilidades de ocurrencia de fuertes lluvias provocadas por inundaciones tienen un papel esencial en el diseño de estructuras relacionadas con el agua y la gestión de recursos hídricos. En muchos casos, los datos para el análisis no están disponibles o son insuficientes para un diseño confiable de dichas estructuras. Con frecuencia se prefiere el análisis de la frecuencia regional con el fin de obtener información para el diseño en sitios donde la disponibilidad de datos es particularmente inadecuada. El presente estudio implementó procedimientos de momentos L para series de precipitación anual máxima de 70 estaciones de medición en la región del Mar Negro medio (MBSR, por sus siglas en inglés), Turquía, para estimar los cuantiles regionales de precipitación. El primer intento de regionalización consistió en evaluar toda el área como una sola región homogénea. Las subregiones se definieron inicialmente con el algoritmo de agrupación en clústeres debido a la presencia de sitios discordantes desde la perspectiva de una región homogénea. De acuerdo con los resultados de las medidas de discordancia y heterogeneidad, se logró la clasificación más adecuada con seis conglomerados (subregiones). Las subregiones cumplen con la condición de homogeneidad como "aceptablemente homogéneas". Se decidió que las distribuciones GEV y GLO en cinco subregiones, la distribución GNO en cuatro subregiones y la distribución PE3 en tres subregiones eran aceptables como distribuciones de frecuencia regional. En comparación, la distribución GPA no es candidata en ninguna de las seis subregiones.

ABSTRACT

The occurrence probabilities of heavy rainfall that cause flood events have an essential role in designing water-related structures and water resource management. In many cases, data for analysis are either not available or are insufficient for reliable design of water-related structures. Regional frequency analysis is usually preferred to provide design information in sites with especially inadequate data available. Our study applied L-moment procedures to annual maximum rainfall series from 70 gauging stations in the Middle Black Sea Region (MBSR) of Turkey to estimate regional rainfall quantiles. The first attempt for regionalization aimed to evaluate the entire area as an homogeneous region. The sub-regions were initially defined with the ward's clustering algorithm due to the presence of discordant sites under a presumption of a single homogeneous region. In compliance with the results of the discordancy and heterogeneity measures, the most promising classification was achieved with six clusters (sub-regions) that satisfied the homogeneity condition as "acceptably homogeneous". It was decided that the GEV and GLO distributions in five sub-regions, the GNO distribution in four sub-regions, and the PE3 distribution in three sub-regions, were acceptable as regional frequency distributions. In comparison, GPA was not a candidate distribution in any of the six sub-regions.

Keywords: maximum rainfall, L-moment, discordancy, heterogeneity measure, index-storm.

1. Introduction

In the context of climate variability, the increasing attention to global warming emerging under the influence of anthropogenic activities has been associated with the consequences of its impacts, which ravage the natural structure of the ecosystem. The IPCC (2007) underlined that the proportional increase of greenhouse gases in the atmosphere would change the conventional climate structure in most parts of the world. It also reported (IPCC, 2013) that heavy rainfall events increased quantitatively towards the end of the 20th century. Hirabayashi and Kanae (2009) reported that more than 300 million people could be affected by even minor floods in 2060-2070. Considering only European countries, economic losses from floods in the next century are expected to rise from € 6.5 billions to € 18 billions (Cetin and Tezer, 2013). Concerning probable extreme precipitation in the future, Giorgi (2006) pointed out that the Mediterranean basin, in which Turkey is located, is among the most vulnerable regions that could be affected by climate change. Previous studies dealing with climate variability in Turkey indicate a remarkable alteration in the characteristics of precipitation (e.g., Turkes and Erlat, 2003; Turkes et al., 2009; Unal et al., 2012; Yurekli, 2015). Regarding precipitation, the most obvious impact of global warming on the world has appeared as floods and droughts, which are the most common and costly natural disasters. Among the probable natural catastrophes in Turkey, floods have caused most deaths and economic losses after earthquakes (Ozcan, 2008). During the period 1948-2015, flood events in Turkey affected 1 778 520 persons and resulted in 1350 fatalities. The economic loss associated with this natural disaster was estimated at USD 2.195 billion (Enginsu, 2015). Ozcan (2006) stated that floods commonly take place in the Black Sea, Marmara, and the Mediterranean regions in Turkey; even the Black Sea region has been exposed to flood events more frequently. Under this study, the Middle Black Sea region experienced 116 flood events in the period from 1956 to 2012, 80 of which occurred in the summer season. These floods caused 29 casualties, 4290 ha of cultivated land damaged, and 8051 homes and working places exposed to undesirable conditions. Seemingly, there has been a substantial increase in the number of floods during the last 15 years in the region (Enginsu, 2015).

Estimation of the magnitude and frequency of heavy rainfall causing floods is of great importance to understand their characteristic behaviour, in order to make decisions on water-related structures (Abolverdi and Khalili, 2010; Shahzadi et al., 2013). A frequent problem regarding the management and planning of water resources for reliable design is to estimate the probable magnitude of extreme rainfall or streamflow events due to the absence of adequate data concerning these events (Yurekli et al., 2009). In this sense, hydrologists have focused for several decades on the reliable analysis of available extreme data in their research (e.g. Kumar et al., 2003; Saf, 2009; Malekinezhad and Garizi, 2014; Ngongondo et al., 2011). The probabilistic characteristic of hydro-meteorologic variables is pivotal in designing water-related structures (Svensson and Rakhecha, 1998). Providing more reliable information about extreme events is crucially important to the management and planning of water resources within a regional context. The accuracy in the design of hydraulic structures is influenced mainly by the adopted frequency analysis approach and the quality and quantity of data used in the analysis.

The availability and quality of hydro-meteorological data is still a severe problem for hydrologists in many parts of the world (Easterling et al., 2000; Haddad et al., 2011; Hussain and Pasha, 2009). In cases where hydro-meteorological data is absent or insufficient in terms of quantity and quality, the regionalization method, referred to as regional frequency analysis, has been frequently used to assess extreme events (Lim and Lye, 2003; Zakaria et al., 2012). This approach consists of identifying the region, finding the sites compatible with each other in a region, applying an homogeneity test for the supposed region, and designating the regional statistical distribution (Sveinsson et al., 2002; Durrans and Kirkby, 2004). The method of L-moments has been widely used in the regionalization of hydrologic data, although there are different approaches for regionalization. Due to their several advantages over conventional moments (Sankarasubramanian and Srinivasan, 1999; Gubareva and Garstman, 2010), the procedure of L-moments has been adopted progressively in hydrologic studies by many researchers since the introduction of the approach (Abolverdi and Khalili, 2010; Modarres, 2010; Zakaria and Shabri, 2013; Anilan et al., 2015;

Mosaffaie, 2015; Sarmadi and Shokoohi, 2015; Yin et al., 2015; Serra et al., 2016).

Even though several efforts have been made to perform regional frequency analysis (RFA) of heavy rainfalls on some parts of Turkey (e.g., Anli, 2009; Anli et al., 2009; Yurekli et al., 2009) during the last decades, no comprehensive studies in the Middle Black Sea Region (MBSR) in which destructive flood events have taken place in the last 15 years have been conducted in the context of RFA for extreme rainfalls. In the studies conducted by Yurekli et al. (2009) and Anli et al. (2009), the L-moments approach was applied to the annual maximum rainfall series of the Cekerek basin and Trabzon Province, respectively, whereas Anli (2009) performed this analysis on both the annual maximum and the partial-duration rainfall series for Ankara province. Seçkin and Topcu (2016) investigated the regional distribution behaviour of the annual maximum rainfalls belonging to 53 precipitation stations in Turkey using the L-moments method. It has been decided that the whole study area could be considered as a homogeneous region based on the heterogeneity test and the generalized logistic distribution has been determined as the most suitable distribution for the region. Ghiaei et al. (2018) carried out a regionalization procedure based on L-moments on the annual maximum rainfall datasets with various durations from seven rainfall stations over the Eastern Black Sea Basin in Turkey. The generalized logistic (GLO) and generalized extreme value (GEV) distributions were determined for short-term (5 to 30 min) and long-term datasets (1 to 24 h) to estimate regional quantiles.

The specific objectives of the present study are: (a) to compute L-moments and its ratios; (b) to check the reliability of the data for the RFA; (c) to form groups of sites that satisfy the homogeneity condition; (d) to choose a regional frequency distribution; (e) to obtain L-moment ratio diagrams to select a candidate regional frequency distribution as an alternative way, and (f) to estimate quantiles based on the best fit distribution for the formed homogeneous region.

2. Materials and methods

2.1 Study area and data

Turkey consists of seven geographic regions, one of which is the Black Sea Region, which comprises three sub-sections, namely the Western Black Sea,

Eastern Black Sea and Middle Black Sea. The MBSR lies between 39º-43º N and 34º-38º E (Fig. 1), with an elevation ranging from 2 m (Fatsa county) to 1287 m (Akkus county). The study area covers roughly 43 684 km^2, approximately 5.6% of Turkey's land area (Enginsu, 2015). The MBS has significant plains: Carşamba and Bafra in the coastal area and Niksar, Erbaa, Tasova and Suluova in the inland area. Kizilirmak and Yesilirmak rivers are the main water resources in the MBSR, which is geographically located in both river basins. The MBSR is under the influence of two different climate characteristics: a temperate oceanic climate affecting the coastal area and a continental climate reigning in the inland area. Precipitation amounts show a significant increase from the interior area towards the coastal zone. Annual rainfall varies from 600 to 800 mm in the coastal part, and decreases to 450 mm towards the inland. Heavy rainfall occurs in the coastal areas during autumn, whereas in inland areas it occurs during the spring (Sozer et al., 1990). Most floods in the period 2000-2012 were experienced across the coastal area (Enginsu, 2015). Kosarev et al. (2007) emphasized that large-scale atmospheric systems positioned over Eurasia and the North Atlantic have mainly become influential in the formation of the climate characteristics of the Black Sea.
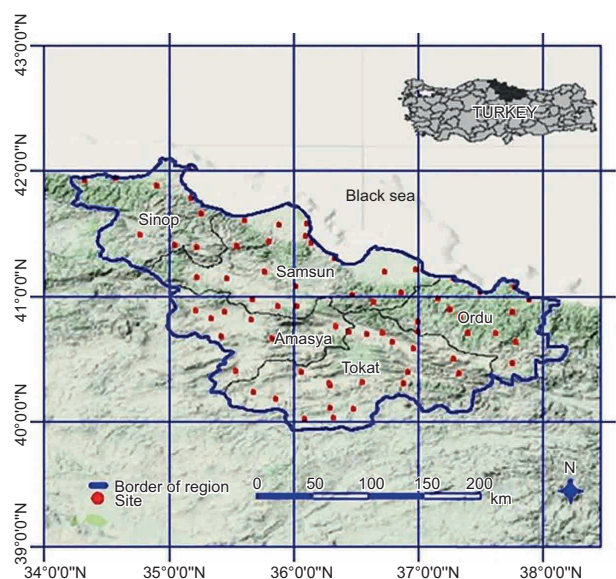

Fig. 1. Geographical location of the stations on the study area.

In the current study, daily rainfall data of 70 recording gauge stations compiled by the Turkish State Meteorological Service and General Directorate of State Hydraulic Works was used. Figure 1 shows the geographical location of the mentioned gauge stations in the study area and preliminary data associated with the sites are given in Table I. However, some recording gauge stations in the MBSR were discarded for a more reliable analysis due to very short record length and questionable data quality. Rainfall datasets belonging to the sites up to 2013 were used for regional frequency analysis in the study, but not every site had an observation length until 2013. There are two methods to choose the maximum rainfall series

Table I. Geographic characteristics of the stations in the study area.

Row	Sample size	Station name	Elevation (m)	Latitude (°N)	Longitude (°E)
1	38	Vezirkopru	377	41.13	35.45
2	20	Alicik	700	40.80	35.31
3	79	Amasya	412	40.65	35.85
4	20	Dogantepe	520	40.60	35.61
5	31	Aydinca	675	40.56	36.15
6	25	Goynucek	530	40.40	35.53
7	39	Gumushacikoy	770	40.88	35.23
8	32	Havza	750	40.96	35.68
9	26	Kavak	741	41.09	36.05
10	47	Ladik	950	40.91	35.91
11	83	Merzifon	755	40.88	35.48
12	39	Suluova	490	40.83	35.65
13	24	Bespinar	721	41.00	35.00
14	53	Mazlumoglu	870	40.54	36.03
15	18	Çakiralan	950	41.00	35.00
16	81	Tokat	608	40.31	36.56
17	60	Turhal	500	40.40	36.10
18	53	Zile	700	40.30	35.90
19	50	Almus	830	40.25	36.56
20	47	Artova	1200	40.05	36.31
21	27	Akkus	1287	40.79	37.01
22	26	Bereketli	1125	40.51	37.30
23	27	Camlibel	1100	40.08	36.48
24	25	Doganyurt	530	40.68	36.71
25	62	Niksar	350	40.60	36.96
26	20	Pazar	540	40.28	36.30
27	30	Resadiye	450	40.16	37.38
28	38	Resadiye / Zile	790	40.13	35.42
29	31	Hacipazari	220	40.43	36.29
30	25	Yolbasi	1050	40.41	37.01
31	31	Ekinli	1070	40.02	36.20
32	30	Sulusaray	950	40.00	36.10
33	44	Tasova	200	40.76	36.33
34	47	Erbaa	230	40.70	36.60
35	12	Camiçi	1250	40.61	37.01
36	50	Dokmetepe	635	40.18	36.20
37	19	Boztepe	750	40.18	35.88
38	27	Turkeli	127	41.94	34.33
39	39	Ayancik	630	41.83	34.77

Table I. Geographic characteristics of the stations in the study area.

Row	Sample size	Station name	Elevation (m)	Latitude (ºN)	Longitude (ºE)
40	25	Erfelek	190	41.87	34.89
41	26	Taflan	150	41.00	36.00
42	24	Duragan	287	41.43	35.05
43	28	Cerçiler	700	41.00	35.00
44	26	Dikmen	385	41.66	35.27
45	21	Kolay	70	41.00	35.00
46	81	Sinop	32	42.02	35.15
47	50	Engiz	25	41.29	36.06
48	29	Gerze	86	41.81	35.17
49	65	Bafra	103	41.55	35.92
50	16	Alacam	7	41.63	35.63
51	48	Boyabat	350	41.46	34.78
52	54	Unye	16	41.14	37.29
53	26	Fatsa	2	41.04	37.48
54	24	Hasanugurlu	120	41.01	36.37
55	84	Samsun	15	41.28	36.33
56	56	Çarşamba	35	41.20	36.73
57	50	Kizilot	10	41.18	36.46
58	34	Terme	10	41.12	37.00
59	26	Duzdag	800	41.01	36.47
60	10	Tekkiraz	550	40.59	37.09
61	23	Kumru	735	40.85	37.24
62	49	Gelemenagri	4	41.40	35.55
63	33	Golkoy	1158	40.69	37.64
64	22	Korgan	725	40.00	37.00
65	24	Topcam	550	40.00	37.00
66	24	Aybasti	632	40.67	37.37
67	35	Mesudiye	1191	40.46	37.77
68	80	Ordu	5	40.98	37.88
69	13	Perşembe	190	40.98	37.70
70	20	Ulubey	190	40.87	37.75

(Anli, 2009). The preferred method is based on selecting the maximum rainfall value of each year. In contrast, the other method (peak-over threshold, POT) is based on choosing all data greater than the considered threshold in a specific period. The overall approach, including selecting the annual maximum rainfall (hereafter referred to as AMR), has been preferred in the current study. The AMR value for daily rainfalls of the corresponding year for every gauge station was obtained.

2.2 L-moments approach

Recently, the L-moments method, popularized by Hosking (1990), has been adopted progressively in frequency analysis of hydro-meteorological variables due to its significant advantages over conventional product moments. Especially, they are relatively insensitive to the presence of outliers in a given series and they have no limits regarding sample sizes. Moreover, they define the structure of any statistical distribution more successfully and estimate the distribution parameters, particularly for hydro-meteorological data in circumstances where individual record lengths at gauging locations are relatively short, and compared with maximum likelihood estimates, they are commonly more tractable about computation. There is no need to transform the available data. On the other hand, compared to product moments, their estimators are almost unbiased, even in small samples, and are near normally distributed (Hosking,

1990; Park et al., 2001; Gubareva and Gartsman, 2010). The properties listed above make them preferable over product moments in frequency analysis of mostly roughly skewed hydro-meteorological data. L-moments are calculated based on probability-weighted moments (PWMs) characterized by Greenwood et al. (1979). A formal definition of the PWMs is provided here:

$$\beta_r = E\left\{X\left[F(X)^r\right]\right\} \tag{1}$$

where $F(x)$ is the cumulative distribution function (cdf) of a random variable X; $X(F)$ is the inverse cfd related to X at F probability level, and r is the rth moment. In Hosking and Wallis (1997), L-moments are defined with regard to the PWMs as:

$$\lambda_{r+1} = \sum_{k=0}^{r}(p_{r,k}^{*}\beta_k) \tag{2}$$

$$p_{r,k}^{*} = -1^{r-k}\binom{k}{r}\binom{r+k}{k} \tag{3}$$

In Eq. (2), λ_{r+1} represents the $(r+1)$th L-moment.

For a given sample $x_1, x_2 \ldots, x_n$, let $x_{1,n} \le x_{2,n} \le \cdots \le x_{n,n}$ represent the order statistics of this series. Analogous to that of Eq. (2), the first four sample L-moments symbolized as l_1, l_2, l_3, l_4 are:

$$l_1 = b_0, \; l_2 = 2b_1 - b_0 \quad l_3 = 6b_2 - 6b_{1+}b_0$$
$$l_4 = 20b_3 - 30b_{2+}12b_1 - b_0 \tag{4}$$

In the Eq. (4,) b_r ($r = 0$, 1 and 2…) is the sample probability weighted moments. Then, sample L-moments ratios, which are t(L-CV), t_3(L-CS), and t_4 (L-CK) are defined as

$$t = l_2 / l_1, \; t_3 = l_3 / l_2, \; t_4 = l_4 / l_2 \tag{5}$$

L-CV, L-CS, and L-CK parameters are coefficients of variation, skewness and kurtosis, respectively.

2.3 Discordancy measure

Based on L-moments, a discordancy measure (D_i) is considered to screen for erroneous data and to check whether or not data are appropriate for achieving the RFA. A station is classified as discordant when its probabilistic behaviour is not like other stations of the region. D_i is calculated based on a vector u_i [t^i, t_3^i, t_4^i]^T, including sample L-moment ratios

(L-CV, L-CS, and L-CK) of a site i (Hosking and Wallis, 1997). The discordancy measure is as follows:

$$D_i = 3^{-1}N\left(u_i - \overline{u}\right)^T S^{-1}\left(u_i - \overline{u}\right) \tag{6}$$

$$S = \sum_{i=1}^{N}\left(u_i - \overline{u}\right)\left(u_i - \overline{u}\right)^T \tag{7}$$

N is the number of sites within the pooling group, and S is a matrix of cross-products. If any site i with $Di > 3$, the site is discordant (Hosking and Wallis, 1993; Rao and Hamed, 2000).

2.4 Regional homogeneity analysis

The heterogeneity (H) test proposed by Hosking and Wallis (1997) is based on the comparison of the between-site variation in the sample L-moments for a tentatively selected region, which has no discordant stations. Therefore, this test estimates the homogeneity degree in a group of sites. Three heterogeneity measures, named H_1, H_2, and H_3 are obtained by considering dispersion measures: L-CV, L-CS and L-CK. These H statistics depend on the 500 homogeneous regions simulated by population parameters equivalent to the regional average of L-moment ratios of the formed region sites (Hosking and Wallis, 1997; Tallaksen et al., 2004). Heterogeneity test statistics (H_i, for $i = 1,2$ and 3) can be calculated by:

$$H_1 = \frac{V - \mu_v}{\sigma_v}, \quad H_2 = \frac{V_2 - \mu_{v2}}{\sigma_{v2}}, \quad H_3 = \frac{V_3 - \mu_{v3}}{\sigma_{v3}} \tag{8}$$

The values of V, V_2 and V_3 in Eq. (8) are estimated as:

$$V = \left\{\sum_{i=1}^{N}\frac{n_i\left(t^i - t^R\right)^2}{\sum_{i=1}^{N}n_i}\right\}^{\frac{1}{2}} \tag{9}$$

$$V_2 = \sum_{i=1}^{N}n_i\left\{\left(t^i - t^R\right)^2 + \left(t_{3-}^i t_3^R\right)^2\right\}^{1/2}\left[\sum_{i=1}^{N}n_i\right]^{-1} \tag{10}$$

$$V_3 = \sum_{i=1}^{N}n_i\left\{\left(t_{3-}^i t_3^R\right)^2 + \left(t_{4-}^i t_4^R\right)^2\right\}^{1/2}\left[\sum_{i=1}^{N}n_i\right]^{-1} \tag{11}$$

where n_i is the record length at site i, and t, t_3, and t_4 are sample L-moments ratios; t^R, t_3^R and t_4^R are the regional average of sample L-moments ratios, respectively; μ_v and σ_v are the mean and standard

deviation of the V values estimated based on N_{sim}, which represents the simulation data achieved by Monte Carlo simulation. The H-statistic value indicates that the formed region is acceptably homogeneous if $H < 1$, possibly heterogeneous if $1 \leq H < 2$, and definitely heterogeneous if $H \geq 2$.

2.5 Determination of the regional frequency distributions

After statistically confirming the group of sites as a homogeneous region, the best fit distribution to the homogeneous region is chosen by the goodness-of-fit-test (Z^{DIST}), suggested by Hosking and Wallis (1997). This test is carried out based on the difference between the L-CK of the candidate distribution and the average L-CK of a homogeneous region under study. This test is given as:

$$Z^{DIST} = \left(t_4^{DIST} - t_4^R + \beta_4 \right) / \sigma_4 \qquad (12)$$

where $DIST$ represents a candidate probability distribution; t_4^{DIST} is the L-CK value dealing with the simulation for the corresponding distribution; t_4^R is the regional average of the at site L-CKs; β_4 is the bias associated with the regional average of the at site L-CKs, and σ_4 is the standard deviation belonging to the L-CK values based on the simulation data sets. The bias and standard deviation of regional average sample L-CK are calculated as follows:

$$\beta_4 = N_{sim}^{-1} \sum_{m=1}^{N_{sim}} \left(t_4^{[m]} - t_4^R \right) \qquad (13)$$

$$\sigma_4 = \left\{ \left(N_{sim} - 1 \right)^{-1} \sum_{m=1}^{N_{sim}} \left(t_4^{[m]} - t_4^R \right)^2 - N_{sim}^{-1} \beta_4^2 \right\}^{1/2} \qquad (14)$$

where N_{sim} is the number of the simulated regions with N sites, and $t_4^{[m]}$ is the L-CK for the mth simulated region. To simulate 500 regions, close to the formed region, the four-parameter Kappa distribution is recommended to estimate β_4 and σ_4. As highlighted by Hosking and Wallis (1997), the four-parameter Kappa distribution for simulation is preferred due to its capability for representing many distributions. According to their simulation analysis, the 500 value for N_{sim} is generally sufficient. The parameters dealing with the Kappa distribution were estimated by using the regional average L-moment ratios. $|Z^{DIST}| \leq 1.64$ should be for a regional candidate distribution, but

the numerically smallest distribution dealing with the $|Z^{DIST}|$ is taken as the best-fit distribution for the formed homogeneous region.

2.6 Prediction of regional quantiles

The well-known index-flood and index-storm approach in either streamflow or rainfall analysis, first introduced by Dalrymple (1960), has been widely used in regional quantile estimates dealing with environmental data. This procedure is based on the assumption that the sites forming a homogeneous region have an identical statistical distribution apart from index streamflow or rainfall value (a site-specific scaling factor) (Hosking and Wallis, 1997). Due to the use of rainfall data as material in our study, the work of Dalrymple (1960) will be hereafter referred to as the index-storm method. Mathematically, the quantile estimates at site i for a region with N sites are calculated by

$$Q_i(F) = \mu_i q(F) \qquad (15)$$

where μ_i is the index rainfall (a site-specific scaling factor) value for site i; F is the non-exceedance probability, and q is dimensionless distribution function (growth curve).

3. Results and discussion

Before applying the L-moments algorithm to the at-site data sets (AMR, otherwise known as block maxima) from rainfall gauging stations in the MBSR, low-order L-moments and its ratios for each site were calculated (Table II). As the first step for regionalization, the consistency among sites in the initially formed region is checked. The test on discordancy in the study was performed with a discordancy measure to assess whether or not there is inter-site consistency. In this sense, the prevalent attempt in RFA is that the whole study area (MBSR) is initially accepted as a homogeneous region. As seen from Table I, the topographic status of all rainfall gauging stations in the MBSR seems to be an obstacle for the evaluation of the entire area as an homogeneous region. Nevertheless, the above-described L-moments methodology was applied to at-site data sets under a presumption of a single homogeneous region. The results of the discordancy test dealing with a single

Table II. Summary statistics of the sites in the MBSR.

Site	ℓ_1	L-CV	L-CS	L-CK	D_i
Vezirkopru	39.25	0.1709	0.2717	0.2563	0.35
Alicik	29.70	0.1719	0.2076	0.1142	0.31
Amasya	32.56	0.1693	0.1833	0.1547	0.08
Dogantepe	30.49	0.2025	0.2805	0.2280	0.08
Aydinca	36.17	0.1484	0.1799	0.0483	1.20
Goynucek	35.60	0.1426	0.2880	0.1885	1.04
Gumushacikoy	32.50	0.1904	0.1704	0.1190	0.25
Havza	35.30	0.1480	0.1600	0.0660	0.79
Kavak	36.49	0.1122	0.1214	0.1394	0.90
Ladik	48.16	0.1871	0.3251	0.2470	0.38
Merzifon	27.91	0.1791	0.1854	0.1524	0.07
Suluova	30.70	0.1958	0.2827	0.1923	0.12
Bespinar	36.58	0.1671	0.2366	0.2694	0.54
Mazlumoglu	39.86	0.1767	0.1323	0.2394	1.18
Çakiralan	33.81	0.1210	-0.0105	0.0316	1.67
Tokat	29.96	0.1688	0.1762	0.1973	0.21
Turhal	33.98	0.1583	0.2103	0.1948	0.17
Zile	32.50	0.1719	0.2478	0.2560	0.34
Almus	33.47	0.1839	0.2911	0.2275	0.18
Artova	29.06	0.1423	0.0981	0.1163	0.53
Akkus	54.11	0.2091	0.2524	0.1798	0.09
Bereketli	32.10	0.1615	0.2502	0.0022	3.15*
Camlibel	24.97	0.1650	0.2056	0.3596	2.55
Doganyurt	39.24	0.1361	0.1183	0.0890	0.61
Niksar	33.34	0.1612	0.1835	0.1929	0.18
Pazar	28.53	0.1799	0.2904	0.3552	1.49
Resadiye	29.62	0.1435	0.1429	0.1200	0.37
Resadiye / Zile	31.92	0.1702	0.3559	0.2424	1.02
Hacipazari	35.10	0.2232	0.3072	0.2041	0.25
Yolbasi	51.78	0.1722	0.2045	0.0643	0.91
Ekinli	31.33	0.1351	0.1622	0.2643	1.31
Sulusaray	28.81	0.1554	0.2583	0.2469	0.50
Tasova	33.16	0.2313	0.4264	0.3307	1.13
Erbaa	33.98	0.1758	0.3045	0.2417	0.37
Camiçi	39.89	0.1589	0.4046	0.2496	2.21
Dokmetepe	31.65	0.1586	0.2352	0.2665	0.60
Boztepe	36.83	0.1717	0.0825	–0.0204	1.81
Turkeli	52.47	0.2059	0.2802	0.2819	0.42
Ayancik	62.00	0.1551	0.0647	0.0992	0.80
Erfelek	56.10	0.1531	0.1409	0.1591	0.30
Taflan	55.28	0.1705	0.1746	0.1600	0.10
Duragan	30.91	0.1578	0.1009	0.0640	0.67
Cerçiler	37.55	0.1728	0.2864	0.2336	0.29
Dikmen	46.71	0.1116	0.2160	0.1412	1.44
Kolay	52.00	0.2110	0.2935	0.1709	0.29
Sinop	49.91	0.2530	0.3146	0.2368	0.66
Engiz	53.90	0.2489	0.3965	0.3085	0.91
Gerze	49.76	0.2007	0.2197	0.1213	0.30
Bafra	52.38	0.1848	0.1070	0.0892	0.67

ℓ_1: first sample L-moment (mean); D_i: discordancy.
*Discordant site.

Table II. Summary statistics of the sites in the MBSR.

Site	ℓ_1	L-CV	L-CS	L-CK	D_i
Alacam	52.18	0.2593	0.0125	0.0729	5.20*
Boyabat	36.59	0.2574	0.3815	0.1707	1.49
Unye	84.35	0.2660	0.3295	0.1624	1.30
Fatsa	98.11	0.3545	0.4520	0.2591	4.38*
Hasanugurlu	66.47	0.3307	0.4253	0.2706	3.16*
Samsun	55.14	0.2251	0.3381	0.2696	0.38
Çarşamba	63.13	0.1935	0.1424	0.1754	0.54
Kizilot	63.73	0.2364	0.3701	0.2949	0.65
Terme	65.61	0.2095	0.2596	0.2784	0.51
Duzdag	104.35	0.1910	0.1775	0.2020	0.31
Tekkiraz	71.91	0.2046	0.0681	0.2022	2.48
Kumru	53.80	0.2036	0.4561	0.4585	3.22*
Gelemenagri	60.96	0.3152	0.4306	0.3296	2.67
Golkoy	57.67	0.1764	0.1424	0.0629	0.64
Korgan	46.83	0.1509	0.2263	0.2093	0.33
Topcam	42.10	0.1808	0.2835	0.1475	0.54
Aybasti	49.69	0.1673	0.1437	0.0464	0.84
Mesudiye	33.19	0.2080	0.3099	0.1551	0.57
Ordu	69.25	0.2002	0.3115	0.2341	0.19
Perşembe	75.51	0.1451	−0.0601	0.1299	3.42*
Ulubey	73.89	0.2566	0.2663	0.1145	1.39

ℓ_1: first sample L-moment (mean); D_i: discordancy.
*Discordant site.

homogeneous region covering 70 rainfall stations are given in Table II. According to the discordancy measure (D_i) results for each site, there is discordancy for six sites, namely Bereketli, Alacam, Fatsa, Hasanugurlu, Persembe, and Kumru. D values for these sites are bigger than the critical value (D_{critic} = 3.0 for ≥ 15 sites in the region). The test statistic values of heterogeneity measures (H), namely H_1, H_2, and H_3, were estimated as 5.84, 1.80, and 1.06, respectively. About these test values, the region covering 70 sites should be classified as definitely heterogeneous for H_1, and possibly heterogeneous for H_2 and H_3 in terms of homogeneity, respectively. The L-moments procedure was reapplied to the region formed by the remaining sites after removing discordant sites to eliminate their undesirable impact on homogeneity. The second effort produced similar results. The heterogeneity test results for the region with 64 sites indicated that it was definitely heterogeneous for H_1, possibly heterogeneous for H_2, and acceptably homogeneous for H_3. In comparison, four sites (Camici, Camlibel, Tekkiraz, and Gelemenagri)

were discordant with the rest of the group. Hosking and Wallis (1997) highlight that the H_1 statistic has much better discriminative capability than H_2 and H_3 to distinguish homogeneity and heterogeneity. The values of H_2 and H_3 are rarely greater than two even in unpleasantly heterogeneous regions. Therefore, the H_1 statistic was considered when deciding on the homogeneity of a given region in the study. However, the results of the other two heterogeneity measures were also presented in this study.

Based on the results of the first and second attempts on regionalization, the idea of evaluating the entire MBSR as a homogeneous region was disapproved. Similarly, the scatter diagrams of L-moment ratios (the L-CV vs. L-CS and L-CS vs. L-CK) also show that the initial proposal for regionalization is not suitable owing to quite high variability in L-moment ratios of the participating sites (Fig. 2). Then, the judgment from the assumption of one homogeneous region emphasizes that the MBSR should be divided into sub-regions until the homogeneity requirement is satisfied for each sub-region. For this purpose, the
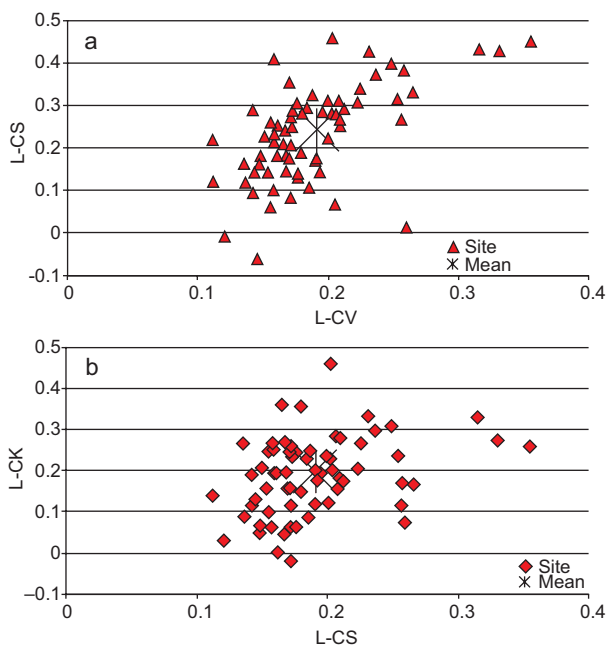
Fig. 2. Position of L-moment ratios with respect to each other for 70 sites. (a) L-CV vs. L-CS; (b) L-CS vs. L-CK.

sub-regions were initially defined with the Ward's clustering algorithm, which has been proposed by Hosking and Wallis (1997). The variables of elevation and latitude/longitude location associated with each site were used as a clustering variable in a preliminary determination of sub-regions. The results indicated that there were cases of two or more probable clusters. The inter-site consistency and homogeneity for each probable cluster (group) were checked by the discordancy measure and heterogeneity test. However, most sub-regions from the clustering method could not fulfil the requirement of inter-site consistency and homogeneity in the relevant region. Therefore, the at-site L-moment ratios were also considered together with the clustering approach in forming a homogeneous group. Moreover, the test results of groups ranging from two up to five were not satisfactory in terms of discordancy and homogeneity, except that of six groups. The most promising classification with a clustering approach was achieved by the Ward's method with six clusters. Three of these sub-regions (regions 1, 2, and 5) covered 15, 22, and 11 sites, respectively (Table III). Figure 3 illustrates the final formation of sub-regions in the studied area. Inter-site consistency in the six sub-regions was proved with

discordancy measure whose critical values (D_{critic} = 3.0 for regions I and II, 1.92 for regions III and IV, 2.63 for region V, and 2.14 for region VI) were greater than the D value calculated for each site in the sub-regions. After reaching the judgment concerning the presence of inter-site consistency among sites forming each sub-region, the next step is to evaluate the homogeneity of a given sub-region in which the sites are assumed to have identical frequency distribution. In this study the homogeneity test was performed by applying heterogeneity measure (H_1) to each sub-region (Table IV). The H_2 and H_3 heterogeneity test results are also given in the Table IV. As can be seen from the table, all sub-regions have satisfied the homogeneity condition; in other words, six sub-regions were designated as acceptably homogeneous regarding the H_1 measure.

The final step in RFA is to estimate an appropriate regional frequency distribution for the data of homogeneous sub-regions identified in the previous section. In our study, three-parameter distributions such as the Generalized Logistic (GLO), Generalized Extreme Values (GEV), Generalized Normal (GNO), Pearson Type III (PE3), and Generalized Pareto (GPA) distributions were considered as candidate distributions for sub-regions. Among them, those representing the regional data were determined according to the Z^{DIST} statistic. It was decided that the distributions providing the basic assumption ($|Z^{\text{DIST}}| \leq$ 1.64) dealing with this statistic could be used to make quantile estimates for the relevant region. The fitted regional distributions are given in Table V, where it can be seen that only the SR-II sub-region has a single regional distribution, while in the rest more regional distributions are selected for quantitative estimation. However, when many distributions were determined to be suitable for regional data in a specific region, the one with the smallest Z-statistic was selected as the most suitable. In this context, GEV for regions SR-I and SR-III, GLO for regions SR-II and SR-V were shosen as the most appropriate distributions. On the other hand, both GEV and GNO had the same and smallest Z-statistic value for SR-IV. The SR-VI region reached the smallest Z-statistic value in the GNO distribution. These results emphasize that GEV and GLO perform very well in fitting to the AMR data in the MBSR, so their test results are found to be acceptable in five sub-regions. The GNO distribution

Table III. Homogeneous sub-regions (SR) and results of discordancy for the sites.

SR-I		SR-II		SR-III	
Site	D_i	Site	D_i	Site	D_i
Vezirkopru	0.64	Tokat	0.31	Turkeli	1.22
Alicik	0.38	Turhal	0.08	Ayancik	1.00
Amasya	0.06	Zile	0.13	Erfelek	0.72
Dogantepe	0.71	Almus	0.15	Taflan	0.10
Aydinca	1.21	Artova	0.82	Duragan	1.62
Goynucek	1.69	Akkus	1.22	Cerciler	0.68
Gumushacikoy	1.04	Bereketli	2.33	Dikmen	1.67
Havza	0.68	Camlibel	1.67		
Kavak	1.77	Doganyurt	0.85		
Ladik	0.77	Niksar	0.16		
Merzifon	0.25	Pazar	0.87		
Suluova	0.60	Resadiye	0.50		
Bespinar	0.97	Resadiye/Zile	1.01		
Mazlumoglu	2.02	Hacipazari	1.78		
Cakiralan	2.21	Yolbasi	0.70		
		Ekinli	1.18		
		Sulusaray	0.33		
		Tasova	2.35		
		Erbaa	0.22		
		Camici	2.80		
		Dokmetepe	0.30		
		Boztepe	2.24		

SR-IV		SR-V		SR-VI	
Site	D_i	Site	D_i	Site	D_i
Kolay	0.28	Unye	1.59	Golkoy	0.55
Sinop	0.39	Fatsa	1.20	Korgan	0.92
Engiz	1.34	Hasanugurlu	0.73	Topcam	0.40
Gerze	0.44	Samsun	0.39	Aybasti	1.02
Bafra	1.01	Carsamba	0.68	Mesudiye	0.28
Alacam	1.85	Kizilot	0.29	Ordu	0.90
Boyabat	1.69	Terme	0.19	Persembe	2.11
		Duzdag	0.51	Ulubey	1.81
		Tekkiraz	2.18		
		Kumru	2.36		
		Gelemagri	0.88		

has the second-best performance after that of GEV and GLO due to its adequacy in four sub-regions. In comparison, PE3 is acceptable three sub-regions and GPA is not a candidate distribution in any of the six sub-regions. In many studies on frequency analysis of hydro-meteorological datasets (e.g., Coles, 2001; Katz et al., 2002; Ribatet et al. 2007; Aghakouchak and Nasrollahi, 2010; Obeysekera and Park, 2013; Li et al. 2015; Aziz et al., 2020) it is highlighted that AMR and POT data sequences are compatible with the GEV and GPA distributions, respectively.

Another attempt on distribution selection for a homogeneous region is a graphical approach (L-moment ratio diagram) which provides a quick visual assessment and compares the sample L-moment ratios with their theoretical counterpart (Peel et al.,
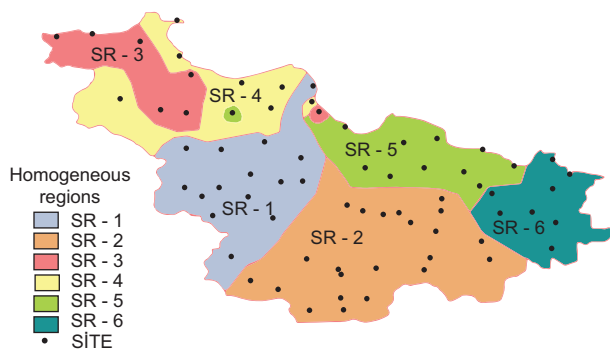
Fig. 3. Final distribution of sub-regions in the study area.

2001). L-moment ratio diagrams (Fig. 4) drawn for each sub-region present similar results to the findings based on the Z^{DIST} statistic. The points denoted by regional average values of L-CV and L-CS on the diagrams were acceptably close to the theoretical curves of distributions fitted to the data in Table V. The proximity to the curve of the candidate distributions included in the current study highlights a probable suitable regional distribution.

The estimation of regional rainfall amounts was accomplished by using the index-storm method given in Eq. (12). By taking the mean annual rainfall of the sub-region as index rainfall for that purpose, the regional rainfall amounts at return periods of 1, 2, 5, 10, 20, 50, and 100 years were obtained based on the corresponding values of growth factors (Table VI). As shown in Table VI, there is no significant difference among the regional AMR values estimated in the -regions where the multiple regional distributions are appropriate, except for the 1-yr return period. According to these results, the distributions found to be acceptable for the sub-regions can be used in the RFA. The choice should be the regional distribution with the minimum $|Z^{DIST}|$, especially for the return periods that lead to differences between estimates.

4. Conclusions

Floods are frequently experienced in the Black Sea region of Turkey. Numerous flood events have taken place in the study area (the MBSR) during the last 70 years. It is imperative to estimate possible future rainfall amounts to avoid floods and minimize their

Table IV. Heterogeneity test results for the six sub-regions.

Heterogeneity measures	SR-I	SR-II	SR-III	SR-IV	SR-V	SR-VI
H1	0.17	−0.46	0.70	0.69	0.94	0.57
H2	−0.73	−0.99	−0.04	2.52*	0.22	0.78
H3	−0.47	−0.48	−0.41	2.06*	−0.34	0.49

*According to H_2 and H_3, the sub- region is definitely heterogeneous.

Table V. Test results based on goodness of fit Z^{DIST} statistic for the six sub-regions.

Homogeneous regions	Candidate distributions				
	GEV	GLO	GNO	GPA	PE3
SR-I	**−0.44**	**1.64**	**−0.94**	−5.21	−1.98
SR-II	−2.02	**−0.15**	−2.73	−6.51	−4.04
SR-III	**−0.36**	**0.96**	**−0.53**	−3.25	**−1.00**
SR-IV	**0.30**	**1.34**	**−0.30**	−2.36	**−1.36**
SR-V	**−1.58**	**−0.86**	−2.28	−3.64	−3.48
SR-VI	**0.72**	1.84	**0.25**	−2.00	**−0.59**

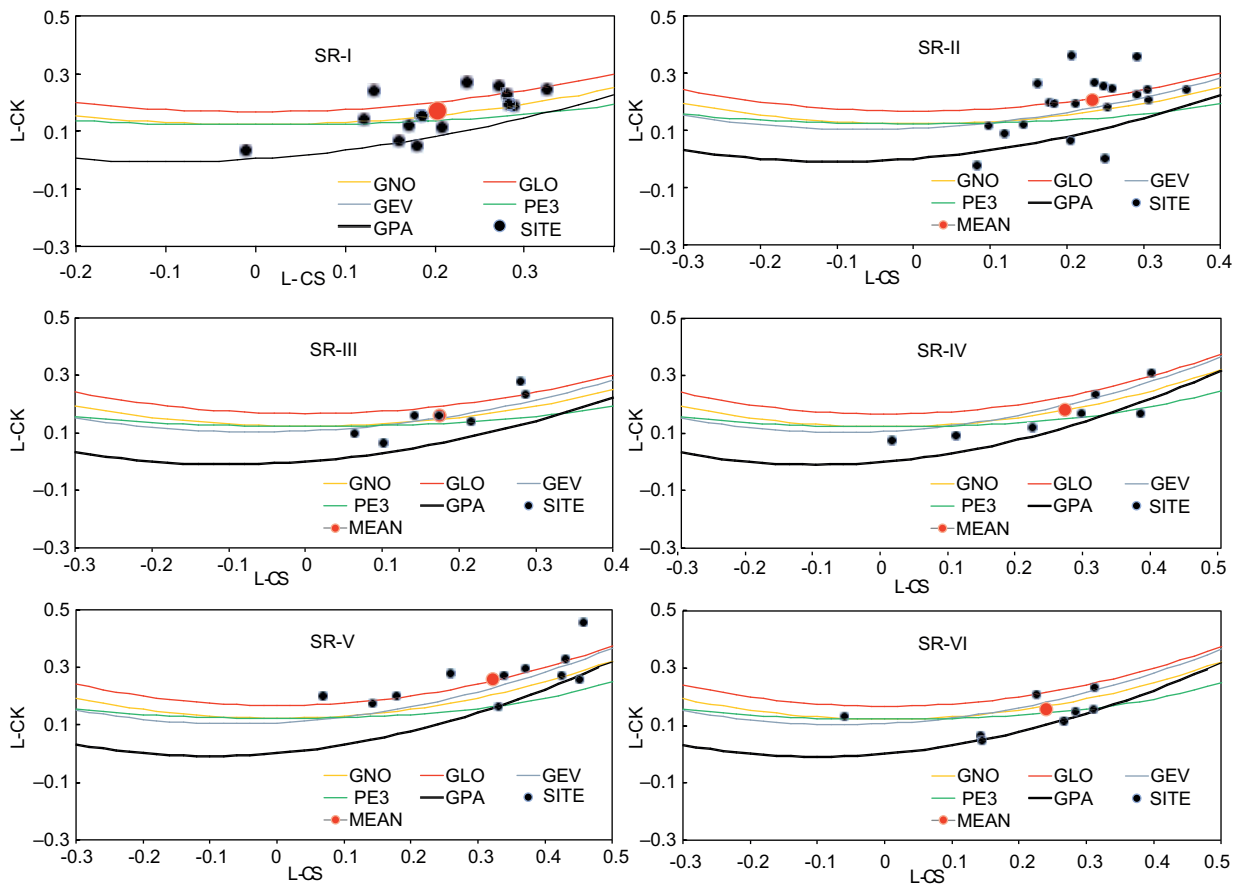Characters in bold show a suitable regional distribution.

Fig. 4. L-moment ratio diagrams of L-CS vs. L-CK associated with SR-I, SR-II, SR-III, SR-IV, SR-V, SR-VI sub-rainfall homogeneous regions.

damages. The amounts in question are also predicted by frequency analysis. The current study was aimed to cope with regional frequency analysis of AMR data sequences by applying the L-moment regionalization procedure. The main conclusions are as follows:

- After initially calculating low-order L-moments and their ratios for 70 sites, the existence of discordant stations to conclude whether or not there is inter-site consistency was checked with discordancy measure for the entire study area in terms of the possibility of forming a single homogeneous region. Six of the 70 sites had discordancy. Additionally, the results associated with the test statistics of three heterogeneity measures ($H1$, $H2$, and $H3$) pointed out that the whole MBSR should be classified as definitely

heterogeneous for $H1$ and possibly heterogeneous for $H2$ and $H3$. These results prove that the region could not be considered as a single homogeneous region. When the MBSR was divided into six sub-regions, each sub-region satisfied the homogeneity test.

- After weighing the inter-site consistency and homogeneity for six sub-regions, the candidate three-parameter distributions were selected based on the goodness of fit Z^{DIST} statistic. The GEV and GLO distributions in five sub-regions, the GNO distribution in four sub-regions, and the PE3 distribution in three sub-regions were found to be acceptable for regional frequency distribution. In comparison, GPA was not a candidate distribution in any of the six sub-regions.

- L-moment ratio diagrams, which are a graphical

Table VI. Annual rainfall amounts estimated from suitable regional distributions.

Region	Distribution	T (years)	1	2	5	10	20	50	100
		F	0.999	0.500	0.200	0.100	0.050	0.020	0.010
SR-I	GEV	q(F)	2.782	0.939	0.743	0.663	0.604	0.546	0.510
		Q(F)	96.9	32.7	25.9	23.1	21.0	19.0	17.8
	GLO	q(F)	3.336	0.944	0.753	0.663	0.593	0.518	0.471
		Q(F)	116.2	32.9	26.2	23.1	20.7	18.0	16.4
	GNO	q(F)	2.709	0.939	0.740	0.661	0.606	0.554	0.523
		Q(F)	94.4	32.7	25.8	23.0	21.1	19.3	18.2
SR-II	GLO	q(F)	3.600	0.937	0.753	0.67	0.606	0.54	0.499
		Q(F)	120.5	31.4	25.2	22.4	20.3	18.1	16.7
SR-III	GEV	q(F)	2.505	0.95	0.756	0.674	0.613	0.553	0.515
		Q(F)	124.4	47.2	37.5	33.5	30.4	27.5	25.6
	GLO	q(F)	3.011	0.954	0.766	0.675	0.602	0.523	0.472
		Q(F)	149.5	47.4	38.0	33.5	29.9	26.0	23.4
	GNO	q(F)	2.487	0.95	0.753	0.672	0.614	0.558	0.524
		Q(F)	123.5	47.2	37.4	33.4	30.5	27.7	26.0
	PE3	q(F)	2.366	0.949	0.749	0.67	0.618	0.57	0.544
		Q(F)	117.5	47.1	37.2	33.3	30.7	28.3	27.0
SR-IV	GEV	q(F)	4.219	0.894	0.656	0.563	0.498	0.434	0.397
		Q(F)	207.8	44.0	32.3	27.7	24.5	21.4	19.6
	GLO	q(F)	5.015	0.901	0.664	0.562	0.485	0.407	0.361
		Q(F)	247.0	44.4	32.7	27.7	23.9	20.0	17.8
	GNO	q(F)	3.872	0.891	0.65	0.562	0.504	0.452	0.423
		Q(F)	190.7	43.9	32.0	27.7	24.8	22.3	20.8
	PE3	q(F)	3.396	0.886	0.638	0.56	0.517	0.486	0.472
		Q(F)	167.3	43.6	31.4	27.6	25.5	23.9	23.2
SR-V	GEV	q(F)	5.304	0.869	0.639	0.554	0.496	0.44	0.407
		Q(F)	364.2	59.7	43.9	38.0	34.1	30.2	28.0
	GLO	q(F)	6.156	0.876	0.645	0.551	0.484	0.418	0.381
		Q(F)	422.8	60.2	44.3	37.8	33.2	28.7	26.2
SR-VI	GEV	q(F)	3.343	0.921	0.714	0.632	0.573	0.516	0.481
		Q(F)	190.4	52.5	40.7	36.0	32.6	29.4	27.4
	GNO	q(F)	3.156	0.919	0.71	0.631	0.577	0.528	0.5
		Q(F)	179.8	52.3	40.4	35.9	32.9	30.1	28.5
	PE3	q(F)	2.858	0.916	0.701	0.629	0.585	0.551	0.536
		Q(F)	162.8	52.2	39.9	35.8	33.3	31.4	30.5

Q(F): Regional rainfall amounts estimated by the index-storm method [$\mu_i\, q(F)$]; q(F): corresponding value of growth factors at different return periods based on the non-exceedance probability; μ_i: index rainfall for site i (regional index rainfall is used for regional quantile estimation); F: probability; T: return period (1/F).

approach to the selection of regional frequency distribution, presented similar results to the findings from the Z^{DIST} statistic.

- The estimation of regional rainfall amounts was performed with the index-storm method. There was no significant difference among the regional AMR values estimated for the sub-regions where the multiple regional distributions are appropriate, except for the 1-yr return period. Nevertheless, the regional distribution with the minimum $|Z^{DIST}|$ should be considered in the regional rainfall quantile estimate, especially for the return periods that lead to differences between estimates.

References

Abolverdi J, Khalili D. 2010. Development of regional rainfall annual maxima for southeastern Iran by L-moments. Water Resources Management 24: 2501-2526. https://doi.org/10.1007/s11269-009-9565-4

Aghakouchak A, Nasrollahi N. 2010. Semi-parametric and parametric inference of extreme value models for rainfall data. Water Resources Management 24: 1229-1249. https://doi.org/10.1007/s11269-009-9493-3

Anilan T, Satilmis U, Kankal M, Yuksek O. 2015. Application of artificial neural networks and regression analysis to L-moments based regional frequency analysis in the Eastern Black Sea Basin, Turkey. KSCE Journal of Civil Engineering 20: 2082-2092. https://doi.org/10.1007/s12205-015-0143-4

Anli AS. 2009. Regional frequency analysis of rainfall data in Ankara province via L-moment methods. Ph.D. thesis. University of Ankara.

Anli AS, Apaydın H, Öztürk F. 2009. Regional frequency analysis of the annual maximum precipitation observed in Trabzon province. Journal of Agricultural Sciences (Turkey) 15: 240-248.

Aziz R, Yucel I, Yozgatligil C. 2020. Non-stationarity impacts on frequency analysis of yearly and seasonal extreme temperature in Turkey. Atmospheric Research 238: 104875. https://doi.org/10.1016/j.atmosres.2020.104875

Çetin NI, Tezer A. 2013. ABD, Avrupa Birliği ve Türkiye'de sel risk yönetiminin karşılaştırılması. 3. Ulusal Taşkın Sempozyumu 29-30 Nisan, İstanbul.

Coles S. 2001. An introduction to statistical modelling of extreme values. Springer, Heidelberg and New York.

Dalrymple T. 1960. Flood frequency methods. Water Supply Paper 1543-A:11-51. U.S. Geological Survey.

Durrans SR, Kirby JT. 2004. Regionalization of extreme precipitation estimates for the Alabama rainfall atlas. Journal of Hydrology 295: 101-107. https://doi.org/10.1016/j.jhydrol.2004.02.021

Easterling DR, Evans JL, Groisman PY. 2000. Observed variability and trends in extreme climate events: A brief review. Bulletin of the American Meteorological Society 81: 417-425. https://doi.org/10.1175/1520-0477(2000)081<0417:OVATIE>2.3.CO;2

Enginsu M. 2015. Regional frequency analysis of daily maximum rainfalls on Middle Black Sea region caused flood. M.Sc. thesis. University of Gaziosmanpasa, Tokat.

Ghiaei F, Kankal M, Anilan T, Yuksek O. 2018. Regional intensity-duration-frequency analysis in the Eastern Black Sea Basin, Turkey, by using L-moments and regression analysis. Theoretical and Applied Climatology 131: 245-257. https://doi.org/10.1007/s00704-016-1953-0

Giorgi F. 2006. Climate change hot-spots. Geophysical Research Letters 33: L08707. https://doi.org/10.1029/2006GL025734

Greenwood JA, Landwehr JM, Matalas NC, Wallis JR. 1979. Probability weighted moments: Definition and relation to parameters of several distributions expressible in inverse form. Water Resources Research 15: 1049-1054. https://doi.org/10.1029/WR015i005p01049

Gubareva TS, Gartsman BI. 2010. Estimating distribution parameters of extreme hydrometeorological characteristics by L-Moment method. Water Resources 37: 437-445. https://doi.org/10.1134/S0097807810040020

Haddad K, Rahman A, Green J. 2011. Design rainfall estimation in Australia: A case study using L-moments and generalized least squares regression. Stochastic Environmental Research and Risk Assessment 25: 815-825. https://doi.org/10.1007/s00477-010-0443-7

Hirabayashi Y, Kanae S. 2009. First estimate of the future global population at risk of flooding. Hydrological Research Letters 3: 6-9. https://doi.org/10.3178/hrl.3.6

Hosking JRM. 1990. L-moments: Analysis and estimation of distributions using linear combinations of order statistics. Journal of the Royal Statistical Society: Series B (Methodological) 52: 105-124. https://doi.org/10.1111/j.2517-6161.1990.tb01775.x

Hosking JRM, Wallis JR. 1997. Regional frequency anal-

ysis: An approach based on L-moments. Cambridge University Press, United Kingdom.

Hosking JRM, Wallis JR. 1993. Some statistics useful in regional frequency analysis. Water Resources Research 29: 271-281. https://doi.org/10.1029/92WR01980

Hussain Z, Pasha GR. 2009. Regional flood frequency analysis of the seven sites of Punjab, Pakistan, using L-moments. Water Resources Management 23: 1917-1933. https://doi.org/10.1007/s11269-008-9360-7

IPCC. 2007. Climate Change 2007: Synthesis Report, contribution of working groups I, II and III to the fourth assessment report of the Intergovernmental Panel on Climate Change. Cambridge University Press, Cambridge.

IPCC. 2013. Climate Change 2013: The physical science basis, contribution of working group I to the fifth assessment report of the Intergovernmental Panel on Climate Change. Cambridge University Press, Cambridge. https://boris.unibe.ch/id/eprint/71452

Katz RW, Parlang MB, Naveau P. 2002. Statistics of extremes in hydrology. Advances in Water Resources 25: 1287-1304. https://doi.org/10.1016/S0309-1708(02)00056-8

Kosarev AN, Arkhipkin VS, Surkova GV. 2007. Hydrometeorological conditions. In: The Black Sea Environment. The handbook of environmental chemistry (Kostianoy AG, Kosarev AN, Eds.). Springer, Berlin, Heidelberg. https://doi.org/10.1007/698_5_086

Kumar R, Chatterjee C, Kumar S, Lohani AK. 2003. Development of regional flood frequency relationships using L-moments for Middle Ganga Plains Subzone 1(f) of India. Water Resources Management 17: 243-257. https://doi.org/10.1023/A:1024770124523

Li LC, Zhang LP, Xia J, Gippel CJ, Wang RC, Zeng SD. 2015. Implications of modelled climate and land cover changes on runoff in the middle route of the south to north water transfer project in China. Water Resources Management 29: 2563-2579. https://doi.org/10.1007/s11269-015-0957-3

Lim YH, Voeller DL. 2009. Regional flood estimations in Red River using l-moment-based index-flood and bulletin 17b procedures. Journal of Hydrologic Engineering 14: 1002-1016. https://doi.org/10.1061/(ASCE)HE.1943-5584.0000102

Malekinezhad H, Garizi AZ. 2014 Regional frequency analysis of daily rainfall extremes using L-moments approach. Atmósfera 27: 411-427. https://doi.org/10.1016/S0187-6236(14)70039-6

Modarres R. 2010. Regional dry spells frequency analysis by L-moment and multivariate analysis. Water Resources Management 24: 2365-2380. https://doi.org/10.1007/s11269-009-9556-5

Mosaffaie J. 2015. Comparison of two methods of regional flood frequency analysis by using L-moments. Water Resources 42: 313-321. https://doi.org/10.1134/S0097807815030112

Ngongondo CS, Xu CY, Tallaksen LM, Alemaw B, Chirwa T. 2011. Regional frequency analysis of rainfall extremes in Southern Malawi using the index rainfall and L-moments approaches. Stochastic Environmental Research and Risk Assessment 25: 939-955. https://doi.org/10.1007/s00477-011-0480-x

Obeysekera J, Park J. 2013. Scenario-based projections of extreme sea levels. Journal of Coastal Research 29: 1-7. https://doi.org/10.2112/JCOASTRES-D-12-00127.1

Ozcan E. 2006. Floods and Turkey. Gazi Egitim Fakultesi Dergisi 26: 35-50 (in Turkish).

Ozcan O. 2008. Evaluation of flood risk analysis in Sakarya river subbasin by using remote sensing and GIS. M.Sc. thesis. Technical University of Istanbul.

Park JS, Jung HS, Kim RS, Oh JH. 2001. Modelling summer extreme rainfall over the Korean Peninsula using Wakeby distribution. International Journal of Climatology 21: 1371-1384. https://doi.org/10.1002/joc.701

Peel MC, Wang QJ, Vogel RM, McMahon TA. 2001. The utility of L-moment ratio diagrams for selecting a regional probability distribution. Hydrological Sciences Journal 46: 147-155. https://doi.org/10.1080/02626660109492806

Rao AR, Hamed KH. 2000. Flood frequency analysis. CRC Press, Boca Raton, FL.

Ribatet M, Sauquet E, Grésillon JM, Ouarda TBMJ. 2007. A regional Bayesian POT model for flood frequency analysis. Stochastic Environmental Research and Risk Assessment 21: 327-339. https://doi.org/10.1007/s00477-006-0068-z

Saf B. 2009. Regional flood frequency analysis using l-moments for the West Mediterranean region of Turkey. Water Resources Management 23: 531-551. https://doi.org/10.1007/s11269-008-9287-z

Sankarasubramanian A, Srinivasan K. 1999. Investigation and comparison of sampling properties of L-moments and conventional moments. Journal of Hydrology 218: 13-34. https://doi.org/10.1016/S0022-1694(99)00018-9

Sarmadi F, Shokoohi A. 2015. Regionalizing precipitation

in Iran using GPCC gridded data via multivariate analysis and L-moment methods. Theoretical and Applied Climatology 122: 121-128. https://doi.org/10.1007/s00704-014-1292-y

Seçkin N, Topçu E. 2016. Regional frequency analysis of annual peak rainfall of Adana and the vicinity. Journal of the Faculty of Engineering and Architecture of Gazi University 31: 1049-1062. https://doi.org/10.17341/gazimmfd.278460

Serra C, Lana X, Burgueño A, Martínez MD. 2016. Partial duration series distributions of the European dry spell lengths for the second half of the twentieth century. Theoretical and Applied Climatology 123: 63-81. https://doi.org/10.1007/s00704-014-1337-2

Shahzadi A, Akhter AS, Saf B. 2013. Regional frequency analysis of annual maximum rainfall in monsoon region of Pakistan using l-moments. Pakistan Journal of Statistics and Operation Research 1: 111-136. https://doi.org/10.18187/pjsor.v9i1.461

Sozer AN, Isik S, Mutluer M. 1990. Agean region geography. Lecture note. Ege University, Izmir, 126 pp.

Sveinsson OGB, Salas JD, Boes DC. 2002. Regional frequency analysis of extreme precipitation in northeastern Colorado and Fort Collins flood of 1997.

Journal of Hydrologic Engineering 7: 49-63. https://doi.org/10.1061/(ASCE)1084-0699(2002)7:1(49)

Svensson C, Rakhecha PR. 1998. Estimation of probable maximum precipitation for dams in the Hongru River catchment, China. Theoretical and Applied Climatology 59: 79-91. https://doi.org/10.1007/s007040050014

Tallaksen LM, Van Lanen HAJ, Eds. 2004. Hydrological drought: Processes and estimation methods for streamflow and groundwater. Elsevier, Amsterdam, 579 pp. (Developments in Water Science, 48).

Turkes M, Erlat E. 2003. Precipitation changes and variability in Turkey linked to the North Atlantic Oscillation during the period 1930-2000. International Journal of Climatology 23: 1771-1796. https://doi.org/10.1002/joc.962

Turkes M, Koc T, Sarıs F. 2009. Spatiotemporal variability of precipitation total series over Turkey. International Journal of Climatology 29: 1056-1074. https://doi.org/10.1002/joc.1768

Unal YS, Deniz A, Toros H, Incecik S. 2012. Temporal and spatial patterns of precipitation variability for annual, wet, and dry seasons in Turkey. International Journal of Climatology 32: 392-405. https://doi.org/10.1002/joc.2274

Yin Y, Chen H, Xu CY, Xu W, Chen C, Sun S. 2015. Spatio-temporal characteristics of the extreme precipitation by L-moment-based index-flood method in the Yangtze River Delta region, China. Theoretical and Applied Climatology 124: 1005-1022. https://doi.org/10.1007/s00704-015-1478-y

Yurekli K, Modarres R, Ozturk F. 2009. Regional daily maximum rainfall estimation for Cekerek Watershed by L-moments. Meteorological Applications 16: 435-444. https://doi.org/10.1002/met.139

Yurekli K. 2015. Impact of climate variability on precipitation in the upper Euphrates-Tigris rivers basin of southeast Turkey. Atmospheric Research 154: 25-38. https://doi.org/10.1016/j.atmosres.2014.11.002

Zakaria ZA, Shabri A, Ahmad UN. 2012. Regional frequency analysis of extreme rainfalls in the west coast of Peninsular Malaysia using partial L-moments. Water Resources Management 26: 4417-4433. https://doi.org/10.1007/s11269-012-0152-8

Zakaria ZA, Shabri A. 2013. Regional frequency analysis of extreme rainfalls using partial L-moments method. Theoretical and Applied Climatology 113: 83-94. https://doi.org/10.1007/s00704-012-0763-2